THE JOURNAL OF PHYSICAL CHEMISTRY C

Article

Cite This: J. Phys. Chem. C 2018, 122, 17954−17962

pubs.acs.org/JPCC

Quantifying the "Subtle Interplay" between Intermolecular and Molecule−Substrate Interactions in Molecular Assembly on Surfaces

Thomas W. White,[†] Natalia Martsinovich,[‡] Alessandro Troisi,[§] and Giovanni Costantini*[,†]

[†]Department of Chemistry, University of Warwick, Coventry CV4 7AL, U.K.

[‡]Department of Chemistry, University of Sheffield, Sheffield S3 7HF, U.K.

[§]Department of Chemistry, University of Liverpool, Liverpool L69 7ZD, U.K.

Supporting Information

ABSTRACT: The effect of the concurrent action of intermolecular and molecule−substrate interactions on the two-dimensional (2D) self-assembly of organic molecules on solid surfaces is investigated in a combined experimental and theoretical effort. Scanning tunneling microscopy measurements of terephthalic acid on the Cu(111) surface, a model system where the interplay between the two interactions is particularly evident, are used to develop a general, simple, and computationally inexpensive model that quantitatively accounts for the experimental observations. The model, related to the well-known Frenkel−Kontorova model, offers a comprehensive description of the "subtle interplay" between intermolecular and molecule−substrate interactions and provides a qualitative and quantitative predictive capability in the design and fabrication of 2D molecular nanostructures at surfaces.

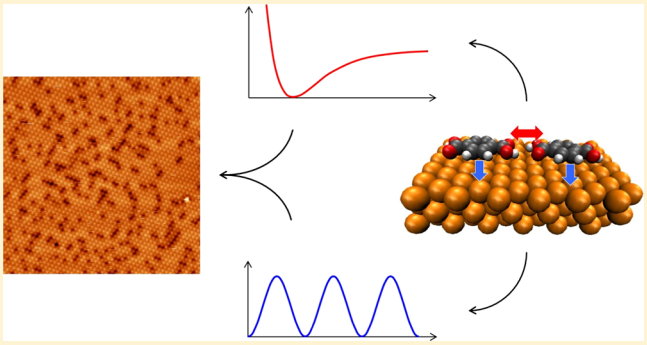

INTRODUCTION

Self-assembly of organic molecules has emerged as a highly effective and versatile strategy for the controlled fabrication of nanoscale structures. Much of its success is owed to recent advances in supramolecular chemistry and organic chemical synthesis. Together, these two complementary disciplines make it possible to design and fabricate molecular building blocks that selectively self-assemble into predetermined functional architectures. The application of this approach to two-dimensional (2D) molecular assembly on solid surfaces,[1−5] however, is not necessarily straightforward, as, in this case, the molecular organization is not determined exclusively by the interactions between the adsorbed molecules. Instead, the substrate often plays an active role, and molecular assembly is driven by a "subtle interplay of intermolecular and molecule−substrate interactions".[6−14]

Despite its importance in supramolecular chemistry on surfaces, the oft-cited "subtle interplay" is not well understood. References to the subtle interplay can be found in the majority of papers on molecular assembly at surfaces but, most frequently, this concept is used only as a sort of general-purpose scapegoat to mask the incapacity to explain specific 2D molecular assembly patterns. In particular, the ability to quantitatively predict the effects of the simultaneous action of intermolecular and molecule−substrate interactions in a general case is yet to be achieved. Therefore, although the successes reported in solution-phase supramolecular chemistry suggest that similar accomplishments should be possible also for molecular self-assembly on solid surfaces, much work is still needed to move from a situation where most of the experimental results are rationalized only a posteriori to the capability of predetermining the final 2D molecular arrangements.

In this work, we have used experimental data acquired on a specific model system—scanning tunneling microscopy (STM) measurements of the assembly of terephthalic acid (TPA, Figure 1a) on the Cu(111) surface—as the starting point to develop a general model of the interplay between intermolecular and molecule−substrate interactions. The model we present here is limited to a one-dimensional (1D) approximation, but the full 2D case will be based on the same fundamental assumptions. Our results show that both a qualitative and quantitative prediction of the experimental molecular assembly is indeed possible, based on a multiscale approach where molecular-level classical and quantum calculations are used to determine input parameters of a computationally inexpensive analytical algorithm operating on large simulation cells.

TPA is an ideal model system for this study, as its assembly has been analyzed on a wide range of different substrates. When deposited onto weakly interacting surfaces such as Au(111), Ag(111), or graphite, either from solution or in vacuum, it remains intact, adsorbs parallel to the surface, and

Received: July 16, 2018
Published: July 19, 2018

DOI: 10.1021/acs.jpcc.8b06797
J. Phys. Chem. C 2018, 122, 17954−17962

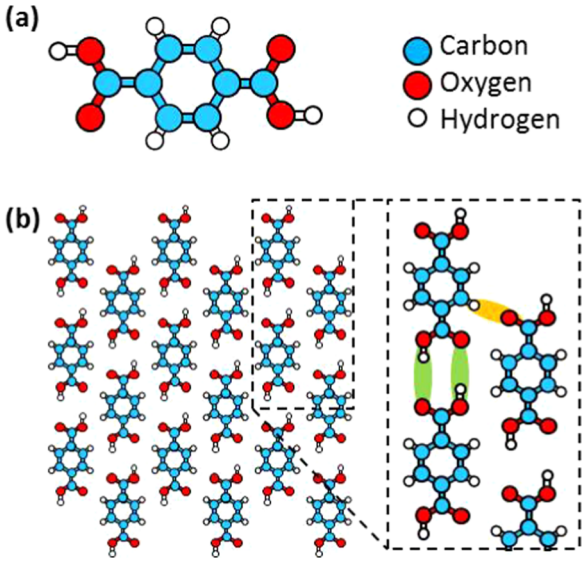

Figure 1. (a) Molecular structure of TPA. (b) Schematic representation of the TPA brickwork supramolecular motif. The zoom-in panel highlights the dimeric hydrogen bonds between carboxylic moieties (green) and the possible secondary bonds involving the aromatic protons (orange).

almost always assembles into the so-called brickwork structure,[15−24] shown schematically in Figure 1b. Here, the carboxyl moieties form dimeric hydrogen bonds with adjacent molecules, resulting in the development of 1D molecular chains that stack in an offset manner to form a brickwork motif. This supramolecular arrangement is also observed in the condensed phase,[25] indicating that, irrespective of the substrate, it is in fact the most energetically favorable structure. The interaction between the TPA chains is believed to be weak, arising from van der Waals interactions and, possibly, secondary electrostatic bonds with the aromatic protons (shown in Figure 1b).[16,17,26] Thus, the assembly in the brickwork phase is essentially 1D in nature. In contrast, when TPA is deposited onto strongly interacting materials like Cu or Pd, or when it is co-deposited with reactive metal adatoms, the carboxyl moiety can deprotonate. The resulting carboxylate species can no longer form standard hydrogen bonds; instead, they assemble into structures characterized by ionic hydrogen bonds[27−31] or coordination bonds to metal adatoms.[31−35] Alternatively, an upright orientation can also be formed, where the TPA binds to the surface through only one carboxylate group.[30,36,37] In such cases, the ultimate arrangement of the molecules does strongly depend on particular aspects of the specific experimental system (i.e., molecule coverage,[38] substrate symmetry, deposition rate,[39] annealing temperature[28]).

The (001) and (110) orientations of Cu single crystals are reactive enough for TPA to deprotonate upon adsorption at room temperature. In particular, on Cu(001), the terephthalate goes on to form a number of different supramolecular architectures, depending on the coverage, which are characterized by ionic hydrogen bonds.[28−30] Similar coverage-dependent phases were also observed on Cu(110), together with the development of metal−organic structures.[31,40] On both surfaces, the supramolecular motifs exhibit symmetries reminiscent of the substrate's atomic structure, indicating a strong molecule−substrate interaction. As Cu(111) is the least reactive Cu termination, it is expected not to deprotonate the adsorbed TPA, although its 2D atomic-scale modulation of the adsorption potential is still expected to influence the molecular assembly.[41]

METHODS

Experimental Methods. All experimental measurements were performed using a commercial ultrahigh-vacuum low-temperature STM instrument. The samples were prepared by multiple cycles of Ar^+ sputtering (1 keV, drain current 14 mA cm^{-2}, 15 min) followed by annealing (870 K, 5 min), which yielded atomically clean and flat terraces. TPA, initially outgassed for several hours at 440 K, was deposited onto the cleaned surface by organic molecular beam epitaxy using a crucible temperature of 450 K, resulting in sub-monolayer coverages after 5−15 min of deposition. The sample was cooled to 77 K prior to insertion into the STM.

The STM measurements were performed using etched W tips that are treated with electron bombardment in the vacuum system. The bias is applied to the sample; thus, positive voltages correspond to tunneling from the tip to the sample, and vice versa. The STM head and sample are held at 77 K throughout measurement. All STM images were processed by using the WSxM software.[42]

Computational Methods. *Molecular Mechanics (MM) Calculations of TPA.* Interaction energies of TPA in the gas phase (i.e., without substrate) were calculated using the MM3 force field[43,44] within the Tinker software;[45] hydrogen bond energy and distance parameters in the MM3 force fields were adjusted to reproduce the acid dimerization energy and the hydrogen bond length obtained using DFT-B3LYP calculations, as described in ref 26: the energy parameter for the O···H interaction was 7.98 kcal mol^{-1} and the distance parameter was 2.05 Å. Energy minimizations were performed for a 1D chain and then for a 2D network of TPA molecules while keeping the z-coordinates of all atoms constant to maintain planarity.

Density Functional Theory (DFT) Calculations of Adsorption. DFT and dispersion-corrected DFT (DFT-D) calculations were performed by using the SIESTA code,[46] within the generalized gradient approximation using the Perdew−Burke−Ernzerhof (PBE) functional,[47] with double-ζ polarized basis sets and pseudopotentials for C, O, Cu, and Au available on the SIESTA web page.[48] Convergence of the Au and Cu bulk and their (111)-oriented slabs was tested; these test results are reported in the Supporting Information (SI).

Calculations of TPA on Cu(111) and Au(111) were done using DFT-D as proposed by Grimme.[49] The dispersion correction was applied only to metal−molecule interactions. Dispersion parameters for the Cu−C, Cu−O, and Cu−H interactions from Grimme's paper were used:[49] C_6 = 45.06, 28.50, and 12.74 eV $Å^{-6}$, R_0 = 3.014, 2.904, and 2.563 Å for Cu−C, Cu−O, and Cu−H pairs, respectively. Dispersion parameters for the Au−C, Au−O, and Au−H interactions were obtained from ref 50: C_6 = 70.89, 44.83, and 20.05 eV $Å^{-6}$, R_0 = 3.112, 3.002, and 2.661 Å for Au−C, Au−O, and Au−H pairs, respectively. S_6 coefficient = 0.75, recommended for PBE,[49] was used. Similarly as for bulk metals, the k-grid cutoff of 15 Å was used, resulting in a 2 × 2 × 1 k-point grid.

Adsorption of TPA (and, for comparison, related molecules: benzoic acid and benzene) on Cu(111) and Au(111) was calculated, first at high-symmetry positions above these surfaces and then on a 2D grid of positions to obtain the

DOI: 10.1021/acs.jpcc.8b06797
J. Phys. Chem. C 2018, 122, 17954−17962

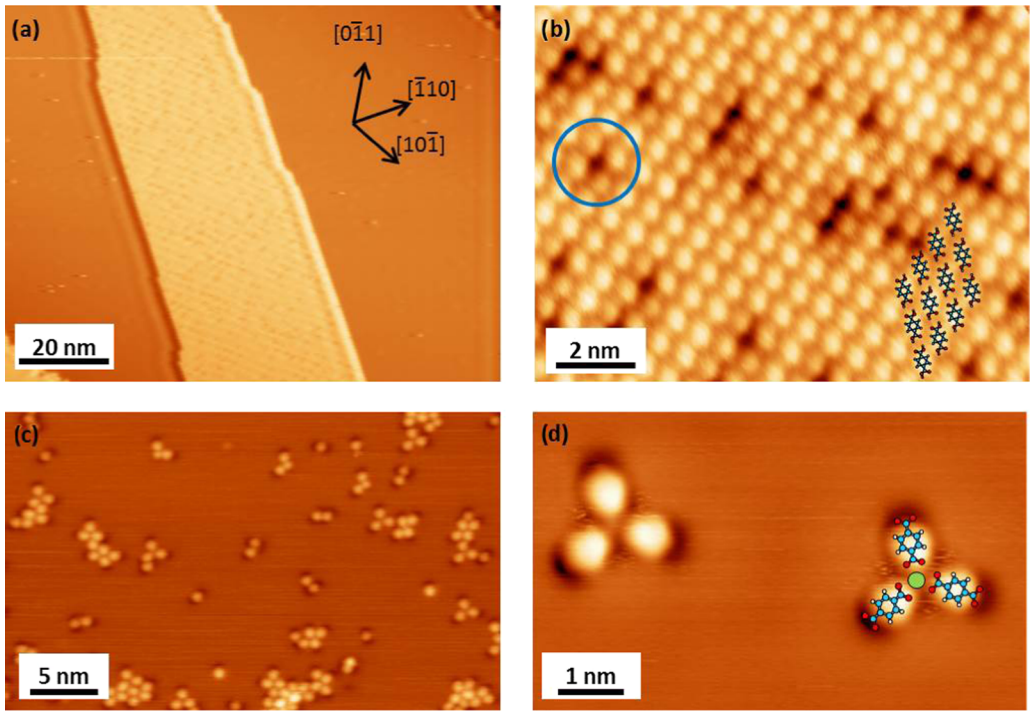

Figure 2. STM images of sub-monolayer TPA deposition on Cu(111). (a) Hydrogen-bonded network. Tunnel current I = 50 pA, sample bias U = 1.3 V. The faint features at the island edges are tip-related artefacts. (b) High-resolution image of the internal structure of the hydrogen-bonded network, demonstrating the distribution of larger gaps between TPA molecules (blue circle). Molecular models of TPA have been overlaid to highlight the molecular orientation. I = 100 pA, U = −1.0 V. (c, d) Molecular arrangement observed after annealing the sample shown in (a) above 350 K. A tentative model of a metal−organic complex has been overlaid in (d). (c) I = 40 pA, U = −1.4 V and (d) I = 50 pA, U = −1.9 V. All images were acquired at 77 K.

potential energy surface (PES) for adsorption of TPA on these surfaces (see the SI for details). Only the metal atoms in the lowest layer of the slab were fixed; the molecule was allowed to optimize both its geometry and position, but there was almost no change in its lateral position during optimization because of the very flat PES. Adsorption energies were calculated as the difference between the energy of the "surface + adsorbate" system and the energies of the clean surface and isolated molecule, and corrected for the basis set superposition error using the counterpoise scheme.[51]

RESULTS AND DISCUSSION

Figure 2 shows typical STM images obtained after depositing sub-monolayer quantities of TPA onto Cu(111). The substrate is held at room temperature during deposition and then cooled to 77 K for imaging. Elongated molecular islands are observed, which exhibit long straight edges, oriented close to the [11$\bar{2}$], [1$\bar{2}$1], and [$\bar{2}$11] substrate orientations (i.e., close to perpendicular to the main substrate orientations[41]).

Detailed inspection of the internal structure of the molecular islands reveals elliptical protrusions that are assigned as individual, flat-lying TPA molecules, in line with previously reported measurements.[15−20,52,53] The overlaid model in Figure 2b reveals two important features of the assembly; the TPA molecules are adsorbed with their long axis aligned parallel to the long edges of the molecular islands and are arranged in a "brickwork-like" structure. Here, we use the term brickwork-like, rather than simply brickwork, due to a number of structural differences that will be discussed later. The supramolecular arrangement of TPA might be taken as an indication of an intact chemical state—i.e., that the molecules have not deprotonated upon adsorption. However, this is not a conclusive proof, as a similar assembly has been reported for deprotonated TPA on Pd(111)[27] and on Cu(001).[54] Verification of the intact carboxyl moiety can be obtained through annealing treatments, which result in a radical transformation of the TPA film. The STM measurements acquired after annealing to 350 K, shown in Figure 2c,d, reveal that the adsorbates are now dispersed over the surface in small aggregates. These aggregates are observed in a range of different motifs, many of which appear to be pinned around a central point. A comparison with previous results in the literature[32,39,55] suggests that the structures in Figure 2c,d are in fact metal−organic complexes, where the central position is most likely occupied by a single Cu adatom (see overlaid model in Figure 2d). Thus, substrate annealing generates metal−organic complexes because it deprotonates the adsorbed TPA molecules and allows the ensuing terephthalate species to bind with Cu adatoms already present as thermally generated defects on the surface. An alternative explanation might be that TPA is already deprotonated in the brickwork-like phase and that annealing is necessary to generate a high enough density of Cu adatoms for complex formation. However, it has been previously demonstrated that the density of thermal adatoms at room temperature on Cu(111) is already sufficiently high to produce metal−organic complexes.[39,56,57] This alternative explanation can thus be excluded, and it can be safely assumed that the brickwork-like structure shown in Figure 2a,b is composed of protonated TPA molecules interacting mainly through hydrogen bonding.

The high-resolution STM image in Figure 2b shows that the TPA hydrogen-bonded monolayer structure developed on

DOI: 10.1021/acs.jpcc.8b06797
J. Phys. Chem. C 2018, 122, 17954−17962

Cu(111) exhibits marked differences to those reported previously on other weakly interacting surfaces.[15−20] Dark spots can be observed in the TPA/Cu(111) lattice, highlighted by the blue circle in Figure 2b, which are only located between the carboxyl moieties. These darker regions are the result of molecules presenting a larger separation from one another along the dimeric hydrogen bonding direction; the molecular separation across these spots is 10.4 ± 0.4 Å (measured as the distance between the centers of two consecutive phenyl rings within the TPA chain), compared to the ∼9.7 Å typically found in hydrogen-bonded TPA chains on other surfaces (a summary of previously reported intermolecular separations in hydrogen-bonded TPA structures on different surfaces can be found in ref 24, 26). On Cu(111), approximately 15% of the intermolecular separations within the hydrogen-bonded chains are elongated in this manner. A statistical analysis of the remaining 85% nonelongated intermolecular distances reveals that they are relatively short, with an average TPA−TPA separation of 9.3 ± 0.02 Å. For example, when compared with the molecular separation in bulk TPA crystals, which is 9.54 Å,[25] the value measured on Cu(111) is 2.5% shorter. This indicates that the hydrogen bonds are being compressed when TPA is adsorbed on Cu(111).[41] On the other hand, the measured interchain separation (i.e., the distance between chains in the direction perpendicular to the dimeric hydrogen bonding direction) is 5.5 ± 0.3 Å, approximately in line with values previously measured for TPA adsorbed onto weakly interacting surfaces.[15−20]

Thus, at variance with what has been reported to date in the extensive literature regarding TPA adsorbed on solid surfaces, the TPA brickwork-like structure on Cu(111) is defective and is characterized by hydrogen bonds that, in their majority (85%), appear to be compressed and, less frequently (15%), elongated. Such an unusual structure seems to indicate an enhanced molecule−substrate interaction that however still preserves the chemistry and intermolecular bonding motif of pristine TPA. As such, the TPA/Cu(111) systems appears to be ideally suited for quantitatively analyzing the interplay of intermolecular and molecule−substrate interactions in supramolecular self-assembly at surfaces. With this aim, we undertook a thorough analysis of the two competing forces using a combination of molecular mechanics (MM) and dispersion-corrected density functional theory (DFT) calculations. The former were employed to investigate the intermolecular interactions and the latter to address the 2D spatial dependence of the molecule−substrate interaction. Finally, the MM and DFT results were combined into a general analytical model, which we use to quantitatively evaluate the effect of the subtle interplay on the molecular assembly.

Figure 3 shows the potential energy calculated by MM as a function of the dimeric hydrogen bond length for an infinite 1D chain of TPA molecules in the gas phase. The distances corresponding to the compressed and elongated intermolecular separations observed on Cu(111) are marked by the red and green lines, respectively. The profile exhibits a Morse-like shape and strongly resembles the one previously calculated by using DFT, with an agreement within 0.1 Å and 0.1 eV.[16] It has a single energetic minimum at 9.65 Å, very similar to the value reported for bulk TPA crystals.[25] However, this is ∼0.3 Å longer and ∼0.8 Å shorter than the compressed and elongated intermolecular separations observed in the TPA/Cu(111) system, respectively. Thus, the MM calculations indicate that

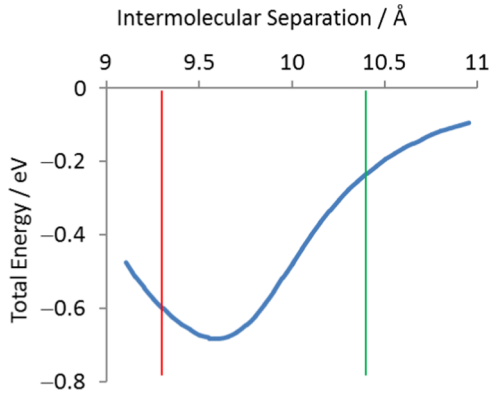

Figure 3. Potential energy calculated by molecular mechanics as a function of the intermolecular separation for an infinite, dimeric hydrogen-bonded 1D TPA chain. The red and green lines correspond to the distances observed on Cu(111) for the compressed and elongated intermolecular separations, respectively.

the formation of compressed and elongated separations in the TPA chains results in energetic penalties of ∼0.1 and ∼0.4 eV, respectively, per dimeric hydrogen bond.

Previous publications suggested that secondary attractive interactions between the aromatic protons and the carboxyl moieties are responsible for interchain binding.[16] To ascertain whether these secondary bonds might possibly induce also the unique assembly of TPA on Cu(111), further MM calculations were performed to identify the lowest-energy configuration of the 1D chains in an infinite 2D network of TPA. The calculations reveal only a single energy minimum with respect to the interchain configuration (see the SI), demonstrating that the interactions between chains cannot cause the compressed and elongated intermolecular separations observed on Cu(111).

To investigate the adsorption energy of a single TPA molecule on Cu(111) as a function of its lateral position on the surface, we utilized dispersion-corrected DFT calculations. We computed the potential energy surface (PES) for the displacement of the molecule oriented along the $[11\bar{2}]$ direction on the substrate (see Figure 4). Equivalent energy minima correspond to the molecule adsorbed with the center of its aromatic ring above the hexagonal close-packed (hcp) hollow site. The hcp position being the lowest energy site is in agreement with computational studies of benzene on (111) metal surfaces.[58,59] Adsorption energies range from −0.77 eV (for the lowest energy adsorption sites) to −0.57 eV (for the highest maximum of the PES). Further computational details and results concerning TPA adsorption energies in several orientations on Cu(111) can be found in the SI. The position of the PES minima of TPA on Cu(111) is similar to that expected for any (111)-terminated metal surface, reflecting the geometric structure of the metal and the molecule. However, the corrugation of the adsorption potential is remarkably high on Cu(111), ∼0.2 eV, e.g., considerably larger than the 0.05 eV calculated for TPA on Au(111) (see the SI). Perhaps surprisingly, most of the adsorption energy arises from the strong interaction between the aromatic ring and the substrate. This is demonstrated by similar DFT calculations that we performed for benzene adsorbed on Cu(111), resulting in an adsorption energy of −0.56 eV, i.e., about 70% of that of TPA (−0.77 eV).

DOI: 10.1021/acs.jpcc.8b06797
J. Phys. Chem. C 2018, 122, 17954−17962

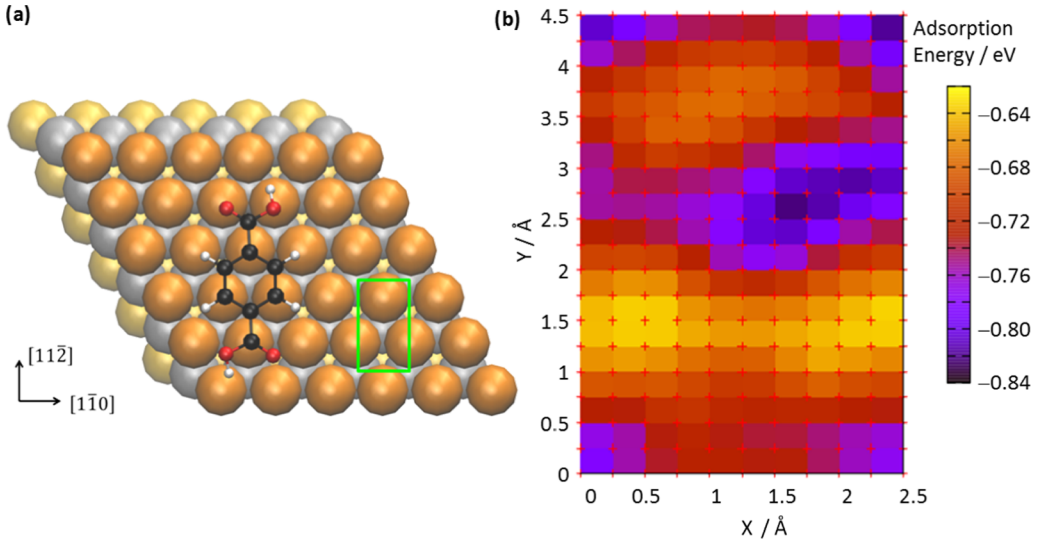

Figure 4. (a) Atomistic model of the most favorable adsorption geometry calculated by dispersion-corrected DFT for TPA on Cu(111). The TPA molecule is positioned with the center of its aromatic ring above a hcp hollow site. (b) Potential energy surface (PES) showing the calculated adsorption energy of TPA on Cu(111) as a function of the molecular position with respect to the atomic substrate lattice. The area of the PES corresponds to the green rectangle shown in (a); *x*- and *y*-coordinates identify the position of the center of the aromatic ring.

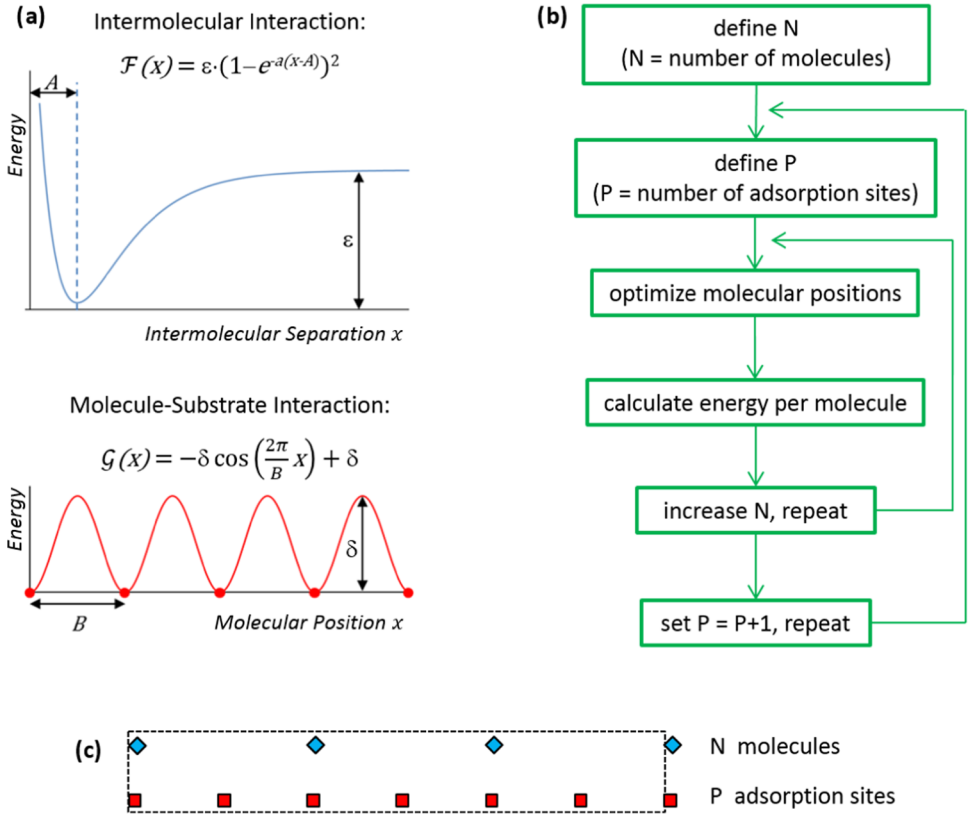

Figure 5. (a) Functions used to approximate the intermolecular and molecule−substrate interactions (see text). (b) Schematic flow diagram of the algorithm used for determining the lowest-energy configuration of the molecular position with respect to the substrate. (c) Example of lowest-energy molecular assembly obtained from the algorithm in (b). The blue diamonds indicate the positions of molecules and the red squares those of the substrate adsorption sites; the simulation unit cell is shown by the dashed line. In this particular example, $P = 6$, $N = 3$, and $\mathcal{L} = A/B = 2.0$.

It is practically very difficult to use DFT calculations to determine the lowest-energy configurations of large islands of molecules adsorbed on surfaces because the supramolecular lattice units and the number of molecules therein are not known in advance. However, it is possible to construct a simple and computationally inexpensive model that describes some general features of the combined effect of intermolecular and molecule−substrate interaction, and that quantitatively accounts for the experimental observations. Indeed, one well-known approach is the Frenkel−Kontorova (FK) model,[60,61] which combines nearest-neighbor interactions and the substrate potential; it has been applied to systems involving

DOI: 10.1021/acs.jpcc.8b06797
J. Phys. Chem. C 2018, 122, 17954−17962

adsorbed atomic layers[62] and molecular layers,[63] epitaxy,[64] and surface reconstruction.[65] Since, in the particular case of TPA on Cu(111), the intrachain bonding is anharmonic, we present here a modified version of the FK model and solve it numerically. Moreover, as the intrachain bonding is significantly stronger than the interchain interactions, our model accounts for the 1D assembly, but it can be extended to describe more general 2D assemblies.

The model is illustrated in Figure 5. We proceed by defining simple but realistic potential energy functions of the intermolecular and molecule−substrate interactions and by computing the lowest-energy molecular arrangement for a variety of system parameters, before considering the specific case of TPA on Cu(111). The intermolecular interaction is modeled by using a Morse function, $\mathcal{F}(x)$, to account for anharmonicity (not included e.g., in the Frenkel−Kontorova model), and the molecule−substrate interaction by a cosine function, $\mathcal{G}(x)$, as depicted in Figure 5a. These are valid approximations because the MM simulations reveal a Morse-like shape for the intermolecular interactions (Figure 3) and the DFT-calculated PES is essentially sinusoidal along the $[11\bar{2}]$ direction (see the SI).

We assume that the lowest-energy arrangement is periodic in 1D with the parameter P defining the number of adsorption sites in the resulting unit cell and N indicating the number of molecules within each unit cell. The values of N and P for the lowest-energy arrangement are not known and we therefore explore a large range of N and P values, computing the lowest-energy molecular arrangement for each of them. The search algorithm is outlined in Figure 5b and described in detail in the SI. Although this algorithm is far from efficient, it fully investigates a large parameter space in a highly systematic manner, allowing the overall lowest-energy configuration to be obtained.

The lowest-energy configuration depends only on the ratio between the characteristic energy well depths of the two interaction potentials, $\mathcal{D} = \epsilon/\delta$, and the ratio of their characteristic distances, $\mathcal{L} = A/B$ (see Figure 5a), and the outcomes of the model are therefore analyzed in terms of these quantities. Before considering the general result, we can inspect a few specific instances. Figure 6a shows the case of a strong molecule−substrate interaction ($\mathcal{D} = 0.5$) and a large mismatch between the spatial modulation B of the substrate adsorption potential and the ideal intermolecular distance A ($\mathcal{L} = 0.4$). The calculated molecular superstructure (shown by the blue diamonds) is clearly strongly perturbed with respect to molecule−molecule separation defined by the intermolecular interactions alone (the "ideal" gas-phase molecular positions are depicted, as a reference, by the green circles): The molecules are in fact arranged in tightly packed pairs centered around the substrate adsorption sites (shown by the red squares). It is important to note that this unusual assembly is a consequence of both the relatively large difference in interaction strengths and the mismatch in the interactions' characteristic lengths. For example, for $\mathcal{D}$ = 0.5, $\mathcal{L}$ = 1.2 (Figure 6b)—which only differs from the case in Figure 6a because of a better spatial commensurability between the molecule−substrate and the intermolecular periodicities—the model predicts a molecular configuration where the adsorbates are uniformly spaced. As one would expect, when $\mathcal{D}$ is increased (i.e., the intermolecular interaction becomes stronger than the molecule−substrate interaction), the lowest-energy arrangement becomes closer to the uniformly spaced configuration that the molecules would assume in the gas phase.

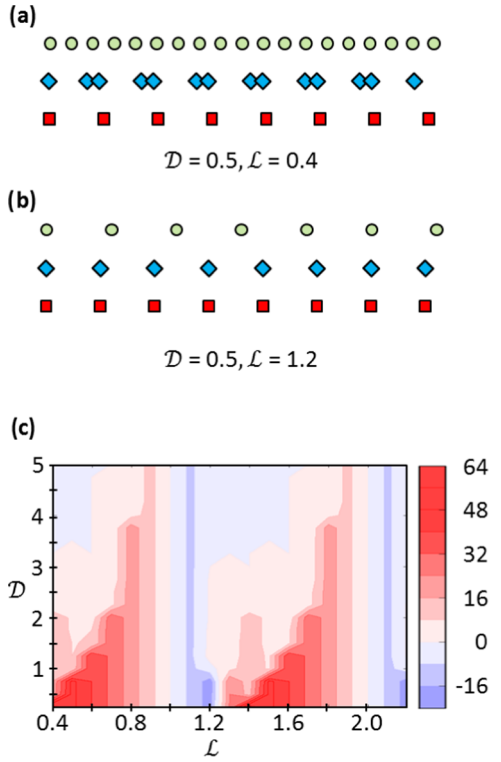

Figure 6. (a, b) Distributions of intermolecular distances determined via the algorithm in Figure 5 for two specific choices of $\mathcal{D}$ and $\mathcal{L}$. The red squares indicate the substrate adsorption sites and the blue diamonds show the calculated lowest-energy molecular positions. The light green circles indicate the location the molecules would have in the gas-phase and are shown as a reference. (a) A case of strong molecule−substrate interaction and strong spatial mismatch and (b) a case of strong molecule−substrate interaction but weak spatial mismatch. (c) Deviation (in %) of the average intermolecular distance from the ideal gas-phase value plotted as a function of the energetic, $\mathcal{D}$, and structural, $\mathcal{L}$, mismatch between the intermolecular and molecule−substrate interactions. The values are given in units of B, the separation between two successive minima in the substrate adsorption potential.

A rapid way to evaluate the overall effect of the substrate on the molecular assembly is to consider the difference between the average intermolecular separation in the gas phase and on the surface. Figure 6c reports this difference as a function of $\mathcal{D}$ and $\mathcal{L}$. Red regions indicate the range of $\mathcal{D}$ and $\mathcal{L}$ where, on average, the intermolecular distances in the 1D adsorbate chains are longer than the gas-phase intermolecular separations, whereas blue regions correspond to an average compression. It is evident that the deviations—i.e., the effect of the interplay between the intermolecular and the molecule−substrate interactions—are most prominent either when the molecule−substrate interaction is very strong ($\mathcal{D}$ is small) or when there is significant incommensurability between the substrate and molecular periodicities.

When the specific parameters determined for the adsorption of TPA on Cu(111) ($\mathcal{D}$ = 3.45 and $\mathcal{L}$ = 2.15) are input into the model, the resulting lowest-energy supramolecular structure is that shown in Figure 7. The calculated intermolecular separation is not uniform but varies continu-

DOI: 10.1021/acs.jpcc.8b06797
J. Phys. Chem. C 2018, 122, 17954−17962

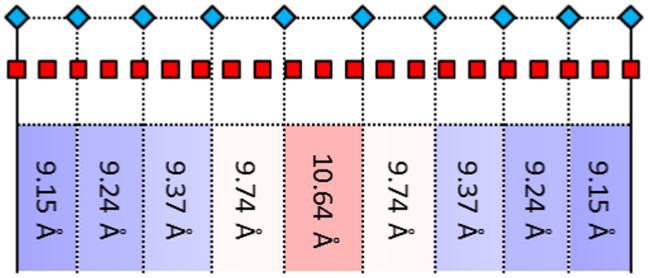

Figure 7. Calculated lowest-energy distribution of TPA molecules on Cu(111) using the algorithm described in Figure 5. The red squares indicate the substrate adsorption sites and the blue diamonds show the calculated lowest-energy molecular positions. The blue and red boxes correspond to molecular separations that are shorter and longer, respectively, than the ideal gas-phase distances.

ously; six out of nine separations (blue boxes) are smaller than the average value, whereas three are larger (red boxes). Critically, the calculated separations closely match those determined experimentally, both qualitatively and quantitatively, whereas the shorter intermolecular distances (9.15−9.37 Å) are consistent with the average measured periodicity (9.3 ± 0.5 Å), one of the nine separations is considerably longer than the others (10.64 Å), in excellent agreement with the experimentally determined intermolecular distance corresponding to the darker spots in Figure 2a (10.4 ± 0.4 Å).

One of the most important aspects of the model presented here is the fact that it can be applied to any molecule-on-substrate system that exhibits a 1D-like self-assembly. To demonstrate its generality, we considered the case of TPA adsorbed on Au(111), which also forms a brickwork structure that, in a first approximation, can be considered as composed of essentially independent 1D TPA chains. For TPA/Au(111), the experimentally observed molecular periodicity is locally uniform with values of 9.9, 10.1, or 10.3 Å, depending on the molecular position with respect to the underlying herringbone reconstruction[16] (i.e., variations occur only over distances of several nanometers). In its present form, our model cannot account for a nonuniform substrate lattice periodicity. However, by using the calculated lattice constant of bulk Au and the calculated PES for TPA on Au(111) (presented in the SI), the input parameters for the TPA/Au(111) system become $\mathcal{D}$ = 13.8 and $\mathcal{L}$ = 1.89, and the corresponding lowest-energy configuration output consists of uniformly spaced molecules separated by 10.22 Å. This is in good agreement with the experimental data reported in ref 16 and confirms that the intermolecular distance for TPA/Au(111) is elongated with respect to both the gas-phase value (9.65 Å, see Figure 3) and the molecular separations in bulk TPA crystals reported in the literature (9.54 Å, ref 25).

One final critical note on the presented model is that the calculations of TPA on Cu(111) suggest the elongated molecular separations should repeat every nine molecules. This is not observed experimentally; although some limited correlation of the dark spots across the molecular lines is apparent in the STM data, the long intermolecular spacings are generally randomly dispersed throughout the molecular lattice (see the SI). This discrepancy is most probably a result of the simplicity of our model. In fact, the optimal configuration shown in Figure 7 has an energy that is very close to that of several other molecular configurations with a similar distribution of intermolecular separations but with different (both slightly smaller and slightly larger) N and P values. As a consequence, because the molecular assembly occurs at room temperature, entropy might play a role alongside enthalpy in determining the final molecular structure. Moreover, a 2D model that includes second-order interchain interactions might reveal more complex supramolecular configurations with only small energetic differences with respect to the most favorable arrangement predicted by the simple 1D version. Although getting into these minor details is beyond the scope of this article, we anticipate that a more refined model that takes into consideration entropic aspects and that includes a full 2D generalization would be based on the same fundamental assumptions and is therefore expected to be qualitatively very similar to the one presented here.

CONCLUSIONS

Efforts to design and construct predetermined 2D supramolecular assemblies on surfaces have, to date, been problematic due to the difficulty in predicting the effects of the interplay between intermolecular and adsorbate−substrate interactions. In this work, based on the experimental analysis of a simple model system where this interplay is particularly evident, we have constructed a general analytical model that allows us to predict the effects of the subtle interplay both qualitatively and quantitatively in a computationally inexpensive manner. It is anticipated that the approach outlined in this work, with its flexibility in the choice of intermolecular and substrate−adsorbate potentials, and its possible extension to include full 2D molecular assemblies and to consider the effect of entropy, will become an important tool for the design of nanostructures on solid surfaces.

ASSOCIATED CONTENT

Supporting Information

The Supporting Information is available free of charge on the ACS Publications website at DOI: 10.1021/acs.jpcc.8b06797.

Details of the numerical model of 1D self-assembly; MM-calculated potential energy surface of 2D arrangements of TPA; DFT-calculated potential energy surfaces for TPA adsorption on Cu(111) and Au(111); distribution of the long intermolecular spacings in the TPA brickwork-like structure obtained from STM measurements (PDF)

AUTHOR INFORMATION

Corresponding Author

*E-mail: g.costantini@warwick.ac.uk. Phone: (+44) 24765 24934.

ORCID

Natalia Martsinovich: 0000-0001-9226-8175
Alessandro Troisi: 0000-0002-5447-5648
Giovanni Costantini: 0000-0001-7916-3440

Notes

The authors declare no competing financial interest.
Data presented in this paper are available at: http://wrap.warwick.ac.uk/106448.

ACKNOWLEDGMENTS

Jennifer McLeod is thanked for insightful comments on this work. G.C. acknowledges financial support from the EU through the ERC Starting Grant "VISUAL-MS" (308115) and

DOI: 10.1021/acs.jpcc.8b06797
J. Phys. Chem. C 2018, 122, 17954−17962

from EPSRC through grant EP/G043647/1. A.T. acknowledges financial support by ERC (Grant No. 615834) and EPSRC (EP/N021754/1). Part of the equipment used in this research was obtained through Birmingham Science City: "Innovative Uses for Advanced Materials in the Modern World" with support from Advantage West Midlands and part funded by the European Regional Development Fund.

REFERENCES

(1) Raval, R. Chiral Expression from Molecular Assemblies at Metal Surfaces: Insights from Surface Science Techniques. *Chem. Soc. Rev.* **2009**, *38*, 707−721.
(2) Barth, J. V. Fresh Perspectives for Surface Coordination Chemistry. *Surf. Sci.* **2009**, *603*, 1533−1541.
(3) Bartels, L. Tailoring Molecular Layers at Metal Surfaces. *Nat. Chem.* **2010**, *2*, 87−95.
(4) Otero, R.; Gallego, J. M.; de Parga, A. L. V.; Martín, N.; Miranda, R. Molecular Self-Assembly at Solid Surfaces. *Adv. Mater.* **2011**, *23*, 5148−5176.
(5) Gooding, J. J.; Ciampi, S. The Molecular Level Modification of Surfaces: From Self-Assembled Monolayers to Complex Molecular Assemblies. *Chem. Soc. Rev.* **2011**, *40*, 2704−2718.
(6) Berner, S.; De Wild, M.; Ramoino, L.; Ivan, S.; Baratoff, A.; Güntherodt, H.-J.; Suzuki, H.; Schlettwein, D.; Jung, T. Adsorption and Two-Dimensional Phases of a Large Polar Molecule: Sub-Phthalocyanine on Ag(111). *Phys. Rev. B* **2003**, *68*, No. 115410.
(7) Stepanow, S.; Lin, N.; Barth, J. V.; Kern, K. Surface-Template Assembly of Two-Dimensional Metal−Organic Coordination Networks. *J. Phys. Chem. B* **2006**, *110*, 23472−23477.
(8) Palermo, V.; Samori, P. Molecular Self-Assembly across Multiple Length Scales. *Angew. Chem., Int. Ed.* **2007**, *46*, 4428−4432.
(9) Kühnle, A. Self-Assembly of Organic Molecules at Metal Surfaces. *Curr. Opin. Colloid Interface Sci.* **2009**, *14*, 157−168.
(10) Elemans, J. A.; Lei, S.; De Feyter, S. Molecular and Supramolecular Networks on Surfaces: From Two-Dimensional Crystal Engineering to Reactivity. *Angew. Chem., Int. Ed.* **2009**, *48*, 7298−7332.
(11) Schnadt, J.; Xu, W.; Vang, R. T.; Knudsen, J.; Li, Z.; Lægsgaard, E.; Besenbacher, F. Interplay of Adsorbate-Adsorbate and Adsorbate-Substrate Interactions in Self-Assembled Molecular Surface Nanostructures. *Nano Res.* **2010**, *3*, 459−471.
(12) Kittelmann, M.; Rahe, P.; Kühnle, A. Molecular Self-Assembly on an Insulating Surface: Interplay between Substrate Templating and Intermolecular Interactions. *J. Phys.: Condens. Matter* **2012**, *24*, No. 354007.
(13) Yang, K.; Xiao, W.; Jiang, Y.; Zhang, H.; Liu, L.; Mao, J.; Zhou, H.; Du, S.; Gao, H.-J. Molecule−Substrate Coupling between Metal Phthalocyanines and Epitaxial Graphene Grown on Ru(0001) and Pt(111). *J. Phys. Chem. C* **2012**, *116*, 14052−14056.
(14) Bathon, T.; Sessi, P.; Kokh, K.; Tereshchenko, O.; Bode, M. Systematics of Molecular Self-Assembled Networks at Topological Insulators Surfaces. *Nano Lett.* **2015**, *15*, 2442−2447.
(15) Kim, Y.-G.; Yau, S.-L.; Itaya, K. In Situ Scanning Tunneling Microscopy of Highly Ordered Adlayers of Aromatic Molecules on Well-Defined Pt(111) Electrodes in Solution: Benzoic Acid, Terephthalic Acid, and Pyrazine. *Langmuir* **1999**, *15*, 7810−7815.
(16) Clair, S.; Pons, S.; Seitsonen, A. P.; Brune, H.; Kern, K.; Barth, J. V. Stm Study of Terephthalic Acid Self-Assembly on Au(111): Hydrogen-Bonded Sheets on an Inhomogeneous Substrate. *J. Phys. Chem. B* **2004**, *108*, 14585−14590.
(17) Lackinger, M.; Griessl, S.; Markert, T.; Jamitzky, F.; Heckl, W. M. Self-Assembly of Benzene−Dicarboxylic Acid Isomers at the Liquid Solid Interface: Steric Aspects of Hydrogen Bonding. *J. Phys. Chem. B* **2004**, *108*, 13652−13655.
(18) Suzuki, T.; Lutz, T.; Payer, D.; Lin, N.; Tait, S. L.; Costantini, G.; Kern, K. Substrate Effect on Supramolecular Self-Assembly: From Semiconductors to Metals. *Phys. Chem. Chem. Phys.* **2009**, *11*, 6498−6504.
(19) Addou, R.; Batzill, M. Defects and Domain Boundaries in Self-Assembled Terephthalic Acid (TPA) Monolayers on Cvd-Grown Graphene on Pt(111). *Langmuir* **2013**, *29*, 6354−6360.
(20) Carrera, A.; Cristina, L. J.; Bengió, S.; Cossaro, A.; Verdini, A.; Floreano, L.; Fuhr, J. D.; Gayone, J. E.; Ascolani, H. Controlling Carboxyl Deprotonation on Cu(001) by Surface Sn Alloying. *J. Phys. Chem. C* **2013**, *117*, 17058−17065.
(21) Song, W.; Martsinovich, N.; Heckl, W. M.; Lackinger, M. Born−Haber Cycle for Monolayer Self-Assembly at the Liquid−Solid Interface: Assessing the Enthalpic Driving Force. *J. Am. Chem. Soc.* **2013**, *135*, 14854−14862.
(22) Yasuda, S.; Furuya, A.; Murakoshi, K. Control of a Two-Dimensional Molecular Structure by Cooperative Halogen and Hydrogen Bonds. *RSC Adv.* **2014**, *4*, 58567−58572.
(23) Laker, Z. P. L.; Marsden, A. J.; De Luca, O.; Della Pia, A.; Perdigão, L. M.; Costantini, G.; Wilson, N. R. Monolayer-to-Thin-Film Transition in Supramolecular Assemblies: The Role of Topological Protection. *Nanoscale* **2017**, *9*, 11959−11968.
(24) Della Pia, A.; Luo, D.; Blackwell, R.; Costantini, G.; Martsinovich, N. Molecular Self-Assembly of Substituted Terephthalic Acids at the Liquid/Solid Interface: Investigating the Effect of Solvent. *Faraday Discuss.* **2017**, *204*, 191−213.
(25) Bailey, M.; Brown, C. The Crystal Structure of Terephthalic Acid. *Acta Crystallogr.* **1967**, *22*, 387−391.
(26) Martsinovich, N.; Troisi, A. Modeling the Self-Assembly of Benzenedicarboxylic Acids Using Monte Carlo and Molecular Dynamics Simulations. *J. Phys. Chem. C* **2010**, *114*, 4376−4388.
(27) Cañas-Ventura, M.; Klappenberger, F.; Clair, S.; Pons, S.; Kern, K.; Brune, H.; Strunskus, T.; Wöll, C.; Fasel, R.; Barth, J. Coexistence of One-and Two-Dimensional Supramolecular Assemblies of Terephthalic Acid on Pd(111) Due to Self-Limiting Deprotonation. *J. Chem. Phys.* **2006**, *125*, No. 184710.
(28) Stepanow, S.; Strunskus, T.; Lingenfelder, M.; Dmitriev, A.; Spillmann, H.; Lin, N.; Barth, J.; Wöll, C.; Kern, K. Deprotonation-Driven Phase Transformations in Terephthalic Acid Self-Assembly on Cu(100). *J. Phys. Chem. B* **2004**, *108*, 19392−19397.
(29) Fuhr, J. D.; Carrera, A.; Murillo-Quirós, N.; Cristina, L. J.; Cossaro, A.; Verdini, A.; Floreano, L.; Gayone, J. E.; Ascolani, H. Interplay between Hydrogen Bonding and Molecule−Substrate Interactions in the Case of Terephthalic Acid Molecules on Cu(001) Surfaces. *J. Phys. Chem. C* **2013**, *117*, 1287−1296.
(30) Tait, S. L.; Lim, H.; Theertham, A.; Seidel, P. First Layer Compression and Transition to Standing Second Layer of Terephthalic Acid on Cu(100). *Phys. Chem. Chem. Phys.* **2012**, *14*, 8217−8223.
(31) Wang, Y.; et al. Varying Molecular Interactions by Coverage in Supramolecular Surface Chemistry. *Chem. Commun.* **2012**, *48*, 534−536.
(32) Wang, Y.; Fabris, S.; Costantini, G.; Kern, K. Tertiary Chiral Domains Assembled by Achiral Metal-Organic Complexes on Cu(110). *J. Phys. Chem. C* **2010**, *114*, 13020−13025.
(33) Clair, S.; Pons, S.; Fabris, S.; Baroni, S.; Brune, H.; Kern, K.; Barth, J. V. Monitoring Two-Dimensional Coordination Reactions: Directed Assembly of Co-Terephthalate Nanosystems on Au(111). *J. Phys. Chem. B* **2006**, *110*, 5627−5632.
(34) Skomski, D.; Abb, S.; Tait, S. L. Robust Surface Nano-Architecture by Alkali−Carboxylate Ionic Bonding. *J. Am. Chem. Soc.* **2012**, *134*, 14165−14171.
(35) Lingenfelder, M. A.; Spillmann, H.; Dmitriev, A.; Stepanow, S.; Lin, N.; Barth, J. V.; Kern, K. Towards Surface-Supported Supramolecular Architectures: Tailored Coordination Assembly of 1, 4-Benzenedicarboxylate and Fe on Cu(100). *Chem. - Eur. J.* **2004**, *10*, 1913−1919.
(36) Martin, D.; Cole, R.; Haq, S. Creating a Functionalized Surface: The Adsorption of Terephthalic Acid onto Cu(110). *Phys. Rev. B* **2002**, *66*, No. 155427.
(37) Tekiel, A.; Prauzner-Bechcicki, J. S.; Godlewski, S.; Budzioch, J.; Szymonski, M. Self-Assembly of Terephthalic Acid on Rutile

DOI: 10.1021/acs.jpcc.8b06797
J. Phys. Chem. C 2018, 122, 17954−17962

TiO_2(110): Toward Chemically Functionalized Metal Oxide Surfaces. *J. Phys. Chem. C* **2008**, *112*, 12606−12609.
(38) Liu, J.; Lin, T.; Shi, Z.; Xia, F.; Dong, L.; Liu, P. N.; Lin, N. Structural Transformation of Two-Dimensional Metal−Organic Coordination Networks Driven by Intrinsic in-Plane Compression. *J. Am. Chem. Soc.* **2011**, *133*, 18760−18766.
(39) Sirtl, T.; Schlögl, S.; Rastgoo-Lahrood, A.; Jelic, J.; Neogi, S.; Schmittel, M.; Heckl, W. M.; Reuter, K.; Lackinger, M. Control of Intermolecular Bonds by Deposition Rates at Room Temperature: Hydrogen Bonds Versus Metal Coordination in Trinitrile Monolayers. *J. Am. Chem. Soc.* **2013**, *135*, 691−695.
(40) Wang, Y.; Lingenfelder, M.; Fabris, S.; Fratesi, G.; Ferrando, R.; Classen, T.; Kern, K.; Costantini, G. Programming Hierarchical Supramolecular Nanostructures by Molecular Design. *J. Phys. Chem. C* **2013**, *117*, 3440−3445.
(41) Clair, S. *Investigation of Low-Dimensional Supramolecular Architectures by Low-Temperature Scanning Tunneling Microscopy*; Ecole Polytechnique Fédérale de Lausanne (EPFL), 2004.
(42) Horcas, I.; Fernández, R.; Gomez-Rodriguez, J.; Colchero, J.; Gómez-Herrero, J.; Baro, A. Wsxm: A Software for Scanning Probe Microscopy and a Tool for Nanotechnology. *Rev. Sci. Instrum.* **2007**, *78*, No. 013705.
(43) Allinger, N. L.; Yuh, Y. H.; Lii, J. H. Molecular Mechanics. The Mm3 Force Field for Hydrocarbons. 1. *J. Am. Chem. Soc.* **1989**, *111*, 8551−8566.
(44) Lii, J. H.; Allinger, N. L. Directional Hydrogen Bonding in the Mm3 Force Field: Ii. *J. Comput. Chem.* **1998**, *19*, 1001−1016.
(45) Ponder, J. W.; Richards, F. M. An Efficient Newton-Like Method for Molecular Mechanics Energy Minimization of Large Molecules. *J. Comput. Chem.* **1987**, *8*, 1016−1024.
(46) Soler, J. M.; Artacho, E.; Gale, J. D.; García, A.; Junquera, J.; Ordejón, P.; Sánchez-Portal, D. The Siesta Method for Ab Initio Order-N Materials Simulation. *J. Phys.: Condens. Matter* **2002**, *14*, 2745−2779.
(47) Perdew, J. P.; Burke, K.; Ernzerhof, M. Generalized Gradient Approximation Made Simple. *Phys. Rev. Lett.* **1996**, *77*, 3865−3868.
(48) https://departments.icmab.es/leem/siesta/Databases/Pseudopotentials/periodictable-gga-abinit.htm.
(49) Grimme, S. Semiempirical Gga-Type Density Functional Constructed with a Long-Range Dispersion Correction. *J. Comput. Chem.* **2006**, *27*, 1787−1799.
(50) Jalkanen, J.-P.; Halonen, M.; Fernández-Torre, D.; Laasonen, K.; Halonen, L. A Computational Study of the Adsorption of Small Ag and Au Nanoclusters on Graphite. *J. Phys. Chem. A* **2007**, *111*, 12317−12326.
(51) Boys, S. F.; Bernardi, F. The Calculation of Small Molecular Interactions by the Differences of Separate Total Energies. Some Procedures with Reduced Errors. *Mol. Phys.* **1970**, *19*, 553−566.
(52) Suzuki, T.; Lutz, T.; Costantini, G.; Kern, K. Terephthalic Acid Adsorption on Si(111)-(Root 3× Root 3)-Bi Surfaces: Effect of Bi Coverage. *Surf. Sci.* **2011**, *605*, 1994−1998.
(53) Stepanow, S.; Lin, N.; Payer, D.; Schlickum, U.; Klappenberger, F.; Zoppellaro, G.; Ruben, M.; Brune, H.; Barth, J. V.; Kern, K. Surface-Assisted Assembly of 2d Metal−Organic Networks That Exhibit Unusual 3-fold Coordination Symmetry. *Angew. Chem.* **2007**, *119*, 724−727.
(54) Argañaraz, B. Q.; Cristina, L.; Rodríguez, L. M.; Cossaro, A.; Verdini, A.; Floreano, L.; Fuhr, J.; Gayone, J. E.; Ascolani, H. Ubiquitous Deprotonation of Terephthalic Acid in the Self-Assembled Phases on Cu(100). *Phys. Chem. Chem. Phys.* **2018**, *20*, 4329−4339.
(55) Pawin, G.; Wong, K. L.; Kim, D.; Sun, D.; Bartels, L.; Hong, S.; Rahman, T. S.; Carp, R.; Marsella, M. A Surface Coordination Network Based on Substrate-Derived Metal Adatoms with Local Charge Excess. *Angew. Chem., Int. Ed.* **2008**, *47*, 8442−8445.
(56) Matena, M.; Stöhr, M.; Riehm, T.; Björk, J.; Martens, S.; Dyer, M. S.; Persson, M.; Lobo-Checa, J.; Müller, K.; Enache, M. Aggregation and Contingent Metal/Surface Reactivity of 1, 3, 8, 10-Tetraazaperopyrene (Tapp) on Cu(111). *Chem. - Eur. J.* **2010**, *16*, 2079−2091.
(57) Berland, K.; Einstein, T.; Hyldgaard, P. Rings Sliding on a Honeycomb Network: Adsorption Contours, Interactions, and Assembly of Benzene on Cu(111). *Phys. Rev. B* **2009**, *80*, No. 155431.
(58) Chwee, T. S.; Sullivan, M. Adsorption Studies of C6h6 on Cu(111), Ag(111), and Au(111) within Dispersion Corrected Density Functional Theory. *J. Chem. Phys.* **2012**, *137*, No. 134703.
(59) Liu, W.; Ruiz, V. G.; Zhang, G.-X.; Santra, B.; Ren, X.; Scheffler, M.; Tkatchenko, A. Structure and Energetics of Benzene Adsorbed on Transition-Metal Surfaces: Density-Functional Theory with Van Der Waals Interactions Including Collective Substrate Response. *New J. Phys.* **2013**, *15*, No. 053046.
(60) Kontorova, T.; Frenkel, J. On the Theory of Plastic Deformation and Twinning. *Izv. Akad. Nauk, Ser. Fiz.* **1938**, *1*, 137−149.
(61) Braun, O. M.; Kivshar, Y. S. Nonlinear Dynamics of the Frenkel−Kontorova Model. *Phys. Rep.* **1998**, *306*, 1−108.
(62) Thayer, G. E.; Bartelt, N.; Ozolins, V.; Schmid, A.; Chiang, S.; Hwang, R. Linking Surface Stress to Surface Structure: Measurement of Atomic Strain in a Surface Alloy Using Scanning Tunneling Microscopy. *Phys. Rev. Lett.* **2002**, *89*, No. 036101.
(63) Bocquet, F.; Nony, L.; Mannsfeld, S.; Oison, V.; Pawlak, R.; Porte, L.; Loppacher, C. Inhomogeneous Relaxation of a Molecular Layer on an Insulator Due to Compressive Stress. *Phys. Rev. Lett.* **2012**, *108*, No. 206103.
(64) Tokar, V.; Dreyssé, H. Lattice Gas Model of Coherent Strained Epitaxy. *Phys. Rev. B* **2003**, *68*, No. 195419.
(65) Thürmer, K.; Carter, C.; Bartelt, N.; Hwang, R. Self-Assembly Via Adsorbate-Driven Dislocation Reactions. *Phys. Rev. Lett.* **2004**, *92*, No. 106101.

DOI: 10.1021/acs.jpcc.8b06797
J. Phys. Chem. C 2018, 122, 17954−17962